Multilayered MOEMS Tunable Spectrometer for Fluorescence Lifetime Detection

Joe Fu-Jiou Lo, Pramod Butte, Qiyin Fang, Shih-Jui Chen, Thanassis Papaioanou, Eun-Sok Kim, Martin Gundersen, and Laura Marcu

***Abstract*—Spectral and time-domain fluorescence from biological samples are powerful diagnostic tools. For applications requiring a compact integrated spectrometer, the microoptoelectromechanical system (MOEMS) is an enabling technology. To improve upon previous microspectrometers, a multilayered, folded design is taken here to improve theoretical resolution and throughput. This sub-cm^3 prototype, based on MOEMS piezoelectric diffractive micrograting, demonstrates over 100-nm tuning in the visible range. Moreover, it integrates a microlens with $f = 2.2$ mm within a microoptics package that is fabricated at wafer-level. The microspectrometer capably records both spectral and lifetime information for fluorescence standards fluorescein isothiocyanate (FITC, 2.5 ns) and Rhodamine B (2.9 ns), and also Collagen Type II (2.4 ns).**

***Index Terms*—Microlens, microspectrometer, multilayer, piezoelectric, wafer-level packaging.**

I. Introduction

MINIATURE spectrometers allow spectral detection of optical signals in a wide variety of applications. The current generation of microspectrometers is designed as a balance between performance and size. These designs—electrostatic tunable cavity-based, waveguide spectrometer-based, and Fabry–Pérot filter-based—typically achieve resolution worse than 10 nm, with limited throughput and/or tuning range [1]–[3]. Also, many of the achieved devices are designed for longer wavelengths (i.e., >1 μm, infrared, telecommunication range) [2], not optimized for fluorescence detection. Moreover, the lack of tuning and/or noise rejection in these devices prevents their use in applications requiring fast, high sensitivity detectors. In contrast, the multilayered microoptoelectromechanical system (MOEMS)-tunable design reported here, integrated on a multimode-fiber, is specifically tailored to fast, high-sensitivity time-resolved spectroscopy.

Applications of time-resolved laser-induced fluorescence (TRLIF), using the aforementioned high speed and sensitivity detector, can differentiate fluorescence sources in terms of both spectral and time information. Thus, it is very useful for inhomogeneous samples like biological tissue. This means that the devices can tolerate a broader spectral resolution, so long as they provide tuning for the high sensitivity detectors. This spectral-time compensation is the main reason the microspectrometer (sub-cm^3) with 10-nm resolution, is able to miniaturize a customized rackmount system ($\sim$1 m^3), from our previous work at Cedars Sinai Medical Center [4].

Manuscript received November 18, 2009; revised December 31, 2009; accepted January 08, 2010. First published February 02, 2010; current version published March 10, 2010. This work was supported by NIH Grant R21EB3628 and by the Whitaker Foundation.

J. F. Lo was with Biomedical Engineering, University of Southern California, USA. He is now with the Bioengineering Department, University of Illinois at Chicago, Chicago, IL 60607 USA (e-mail: joef.lo@gmail.com).

P. Butte and T. Papaioanou are with Cedars Sinai Medical Center, Los Angeles, CA 90048 USA (e-mail: pramod.butte@cshs.org; p_thanassis@yahoo.com).

Q. Fang was with Cedars Sinai Medical Center, Los Angeles, CA 90048 USA. He is now with Engineering Physics, McMaster University, ON, L8S 4L7, Canada (e-mail: qiyin.fang@mcmaster.ca).

S.-J. Chen, E.-S. Kim, and M. Gundersen are with the Electrical Engineering and Electrophysics Department, University of Southern California, Los Angeles, CA 90089 USA (e-mail: shihjuic@usc.edu; eskim@usc.edu; mag@usc.edu).

L. Marcu is with Biomedical Engineering Department, University of California, Davis, CA 95616 USA (e-mail: lmarcu@ucdavis.edu).

Color versions of one or more of the figures in this letter are available online at http://ieeexplore.ieee.org.

Digital Object Identifier 10.1109/LPT.2010.2040995

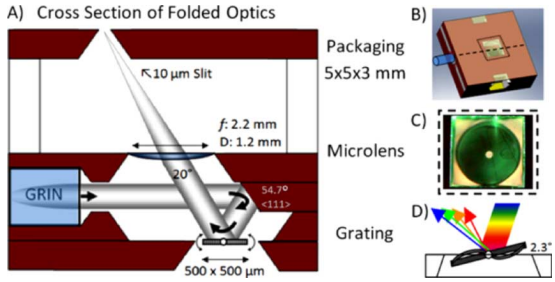

Fig. 1. (A) Cross section of the μSpect. (B) Perspective view of the μSpect ($5 \times 5 \times 3$ mm^3) with gradient index (GRIN) fiber connected from the side. (C) Top view photo of the microlens inside the μSpect. (D) Cross-sectional view of the MOEMS grating. The grating and microlens are also shown in (A).

II. Multilayered Microspectrometer (μSpect) System

MOEMS and miniaturized optical systems typically require compromises between light throughput, spectral resolution, and size (i.e., focal length). In the case of TRLIF, a 10-nm resolution is acceptable, as time resolution compensates spectral resolution. This allows the μSpect to use a short 2.2-mm focal length, while providing 10-nm resolution within visible spectrum, where most endo/exogenous fluorophores and labels emit. The completed μSpect provides an 8-nm scanning with a 450- to 575-nm range in a packaged, $5 \times 5 \times 3$ mm multilayered die. This μSpect design represents a unique solution for time-resolved fluorescence as it balances miniaturization with requirements of optical performance.

The μSpect is a multilayered design based on a tunable spectrometer (Fig. 1), which enables a folded path with larger grating and wider aperture than typical planar designs. The system couples input light via a 10-μm core fiber with a pigtailed gradient index (GRIN) lens. Then, a piezoelectric actuated MOEMS grating separates the different wavelength

1041-1135/$26.00 © 2010 IEEE

Authorized licensed use limited to: McMaster University. Downloaded on June 25,2010 at 19:14:19 UTC from IEEE Xplore. Restrictions apply.

TABLE I
PERFORMANCE COMPARISON OF DIFFERENT SPECTROMETER SYSTEMS

Specifications	Custom	Ocean Optics	10μ Fiber	Micro*	μSpect
F (mm)	320	100	--	~mm	2.2
Resolution (nm)	0.5	1	--	>12	10
NA	0.1	0.11	0.12	--	0.105
Size (cm^3)	54000	500	--	Sub cm^3	0.125
Etendue* (μm^2)	2820	153	3.55	~0.3	2.95
E×R (μm^3)	1.4	0.15	--	0.0036	0.03

*"Micro" system is based on previous microspectrometers cited in this paper.
*Etendue, E, is a combination of optical cross section and half angle

components within the input intensity. It employees integrated microlens (1.2-mm diameter, 2.2-mm f) to focus the separated wavelengths on an exit slit (10 μm), which decreases the noise for low intensity applications. The μSpect is comprised of three main components: 1) MOEMS grating, 2) integrated microlens, and 3) wafer-level packaging. These components are designed together as an integrated microoptics system.

III. DESIGN AND FABRICATION

To design the optics, a geometric comparison was made between the custom spectrometer [4], a portable spectrometer (i.e., Ocean Optics), and microspectrometers. The etendue—geometric extend or theoretical throughput—was used as the criteria for comparison (Table I). As the system size decreased to μSpect (over 400 000 × smaller), the etendue decreased while the numerical aperature (NA) remained similar. However, the reduction would have been worse if not for the resolution broadening to 10 nm (as etendue is $\propto$ resolution). In comparison, the μSpect had throughput advantage over other planar microdevices due to their two-dimensional, reduced NA/etendue. The μSpect was designed to have similar etendue as a 10 μm, NA 0.12 optical fiber. This matching was applied to the input collection fiber to reduce coupling loss and maximize the μSpect throughput.

The MOEMS grating was the key component that provided spectral dispersion and tuning. The MOEMS grating was formed by fabricating four piezoelectric cantilevers (300 μm long, 50 μm wide), arranged in opposing pairs, one going up and one down, to provide rotation of a 500×500 μm diffractive grating (125 l/mm $R = 62$) without displacing the central pivot. Furthermore, 7 μm SU8 was patterned to flatten the grating, as the added mass counters the cantilever curling caused by compressive residual stress of RF sputter-deposited piezoelectric ZnO film. These units were arrayed on silicon substrate, representing one layer of the multilayer.

To collect the diffracted light from the MOEMS grating, a 1.2-mm diameter microlens was fabricated onto a clear, SU8 diaphragm. This diaphragm-suspended microlens represented one of the multilayer in the μSpect. The curvature of the microlens was molded from reflown photoresist (AZ 4620 at 145°C) via an intermediate cast in polydimethylsiloxane (PDMS). With this process, a variety of materials, in this case SU8, could be molded into the microlens diaphragm.

Upon the realization of both MOEMS grating and microlens layers, the multiple layers were aligned and packaged at wafer-level. The layers consisted of the input fiber, Al coated Si plane (111) mirror, grating, and microlens. We measured the efficiency of the (111) mirror to be 95% at 543 nm. Typical roughness (R_a) less than 100 nm for this KOH formed (111) surface was well reported [5]. Because an array of units was

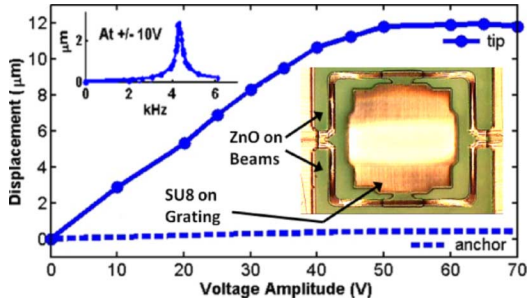

Fig. 2. MOEMS grating displacement at tip versus anchor when actuated by sinusoidal voltage input. The tip had linear actuation up to ±50 V with maximum 12 μm or 2.3° tilting. Top inset: Frequency response with 4.3-kHz fundamental resonance. Bottom inset: Grating with 4 ZnO beams and SU8.

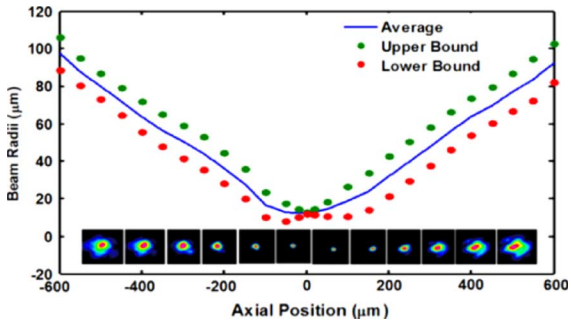

Fig. 3. Measured beam radii as a function of the axial position from the focal point of the microlens. The focal length was measured to be 2.18 mm with M^2 being 2.89. Inset: Photos of the actual focal cross sections as imaged by a CCD profiler, minor surface bending visible (focal length unaffected).

achieved on each wafer, wafer-level packaging combined both batch processing and protective encapsulation. One μSpect die fabricated from the array using wafer-level packaging measured $5 \times 5 \times 3$ mm.

IV. COMPONENT AND SYSTEM PERFORMANCES

For piezoelectric actuation of the MOEMS grating, voltage induced displacement was characterized via a laser Doppler displacement meter (Optodyne). Actuation was induced by applying sine waves at varying peak voltage with varying frequencies (Fig. 2). Linear actuation was obtained with applied voltage up to ±50 V, while maximum displacement was obtained at 4.3 kHz. A total 2.3° of linear actuation (~300-nm spectral equivalent) can be obtained by the actuator.

The fabricated microlens was characterized by its focusing performance. Using a HeNe laser with reduced diameter (0.5 mm) and a charged coupled detector (CCD) beam profiler (Coherent), the focal profiles were recorded. In this manner, the length of focus and the amount of divergence from diffraction limit—or M^2—were calculated (Fig. 3). A focal length of 2.18 mm was achieved by the 1.2-mm diameter microlens with M^2 value of 2.89 (high-quality optics $M^2 \sim 1.3$). The fabricated microlens met the requirements of the focal length in the μSpect system and a low M^2 helped the signal-to-noise ratio by reducing scattering.

The packaged μSpect was characterized by its separation of a collinear dual wavelength laser (543/594 nm, PMS Electrooptics). A reduced, 0.5-mm diameter collinear beam was delivered into the μSpect; and the output was imaged on a CCD imager (Coherent). The 543- and 594-nm bands are well separated in

Authorized licensed use limited to: McMaster University. Downloaded on June 25,2010 at 19:14:19 UTC from IEEE Xplore. Restrictions apply.

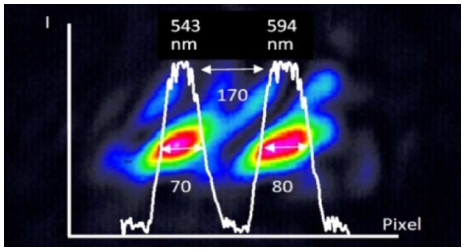

Fig. 4. The packaged μSpect's capability to separate 543- and 594-nm light as imaged on a CCD profiler near the detector plane. The overlay intensity graph showed better than 25-nm resolution (FWHM) in the prototype μSpect.

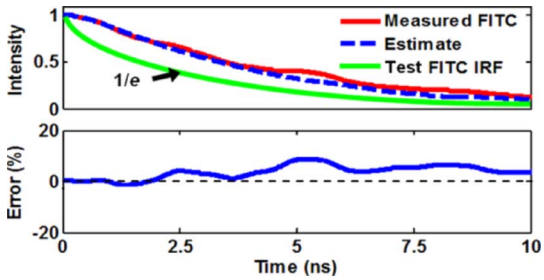

Fig. 5. Example of signal analysis. The μSpect measurement of the FITC decay was deconvolved of the laser pulse. Then, the result was reconvolved and compared to the original measured signal, giving better than 10% error. The $1/e$ lifetime was then calculated from the impulse response function, IRF.

Fig. 4, with a full-width at half-maxima (FWHM) suggesting a 25-nm resolution. The performance could be improved with higher grating resolution, although wider bandwidth benefits throughput (via etendue considerations).

V. Time-Resolved Measurement

The μSpect was mounted to a microchannel plate photomultiplier tube (MCP-PMT, Hamamatsu) for time-resolved measurements. As the μSpect was scanned with 4.3-kHz sinusoid, a pulse generator (SRS) synchronized a fast laser pulse (1.2 ns) over the peak scanning. After the sample was excited and emission was processed by the μSpect, the MCP-PMT gating was opened by a delayed trigger, allowing the time-decay at particular wavelength to be recorded. By operating μSpec at 4.3 kHz, maximum scanning was obtained.

The combined spectral/lifetime signal was averaged over eight traces per wavelength. The fluorescence impulse responses of the samples were then extracted from the raw data with reconvolution, in which a test impulse was reconvolved with the laser pulse as a check against the original signal (Fig. 5). Then, the lifetimes of the impulses were calculated as the time to decrease by e, or 37% of the initial intensity [6].

Fluorescence emissions from three species (FITC, Rhodamine B, and collagen type II) were measured with the μSpect. The 100-μM FITC and Rhodamine were prepared in Tris and ethanol, respectively. Dry collagen II powder from bovine cartilage (mimic tissue matrix) was also used to test the μSpect. The prototype μSpect provided a limited scanning range of 450–575 nm. However, the red-shifted and blue-shifted spectra of Rhodamine and collagen were visible, and the peak FITC emission (520 nm) was resolvable (Fig. 6).

In addition, lifetimes of FITC, Rhodamine, and collagen II were measured at 2.5, 2.9, and 2.4 ns, respectively. These

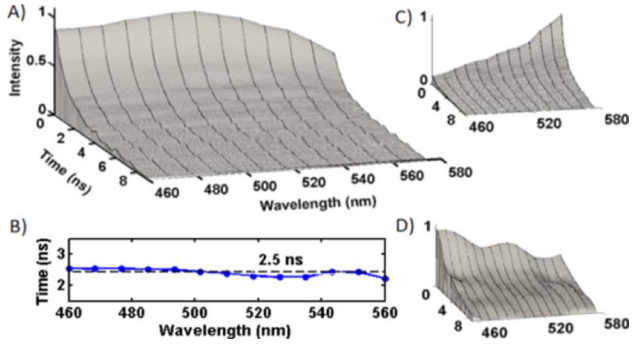

Fig. 6. TRLIF measurement with μSpect. (A) On FITC with maximum fluorescence at 520 nm. (B) FITC showed almost constant lifetime over scanned wavelength span. (C) On Rhodamine B with a maximum fluorescence above 600 nm. (D) On collagen with a maximum fluorescence below 390 nm.

values, while sensitive to solvent conditions, were consistent with reports in various systems and imaging techniques [4], [7], at the experimental concentrations.

VI. Discussion and Improvements

A 25-nm bandwidth MOEMS spectrometer scanned at 8 nm with a range of 450–575 nm was demonstrated in this report. Using this device, we differentiated spectral and lifetime fluorescence between FITC, Rhodamine B and collagen. However, the prototype device performance can be improved: The scanning range, hindered by thin film stress, can be improved by stiffer structural materials (i.e., Al_3O_2) or stress compensation. The optical resolution can be enhanced by higher grating power. Better wafer handling via aligner/bonder can increase throughput by minimizing optical misalignments.

In comparison, μSpect's resolving power R can be upgraded above competing devices ($R = 60$), surpassing 10-nm resolution. Also, 3-D multilayered structure of μSpect allows a long focal path (folded) to be combined with higher etendue, representing the most efficient use of the sub-cm^3 device size. The μSpect proof-of-concept shows that MOEMS can uniquely compliment spectroscopy at the microscale level. Our result gives motivation for the increasingly popular integrations of multiple time/spectral and other sensing modalities in space-limited minimally invasive biomedical applications like microsurgery and tissue diagnosis.

References

[1] R. F. Wolffenbuttel, "MEMS-based optical mini- and microspectrometers for visible and infrared spectral range," *J. Micromech. Microeng.*, vol. 15, pp. 145–152, 2005.
[2] E. Shields, W. Zhou, Y. Wang, and J. Leger, "Microelectromechanical system-based adaptive space-variant imaging microspectrometer," *Appl. Opt.*, vol. 46, no. 31, pp. 7631–7639, 2007.
[3] P. Cheben *et al.*, "A high-resolution SOI arrayed waveguide grating microspectrometer with submicrometer aperture waveguides," *Opt. Express*, vol. 15, no. 5, pp. 2299–2306, 2007.
[4] Q. Fang, T. Papaioannou, J. A. Jo, R. Vaitha, K. Shastry, and L. Marcu, "Time-domain laser-induced fluorescence spectroscopy apparatus for clinical diagnosis," *Rev. Sci. Inst.*, vol. 75, no. 1, pp. 151–162, 2004.
[5] S. S. Yun, S. K. You, and J. H. Lee, "Fabrication of vertical optical plane using DRIE and KOH crystalline etching of (110) silicon wafer," *Sens. Actuators A*, vol. 128, pp. 387–394, 2005.
[6] J. Jo *et al.*, "Laguerre based method for analysis of time-resolved fluorescence data," *J. Biomed. Opt.*, vol. 11, no. 2, pp. 021004-1–13, 2006.
[7] A. Imhof, M. Megens, J. J. Engleberts, D. T. N. de Lang, R. Sprik, and W. L. Vos, "Spectroscopy of fluorescein (FITC) dyed colloidal silica sphers," *J. Phys. Chem. B*, vol. 103, pp. 1408–1415, 1999.

Authorized licensed use limited to: McMaster University. Downloaded on June 25,2010 at 19:14:19 UTC from IEEE Xplore. Restrictions apply.